Computers and Concrete, *Vol. 18, No. 2 (2016) 267-278*
DOI: http://dx.doi.org/10.12989/cac.2016.18.2.267

Damage and fracture processes of concrete using acoustic emission parameters

Fan Xiangqian[1,2*], Hu Shaowei[1,2] and Lu Jun[1,2]

[1]*Department of Materials and Structural Engineering, Nanjing Hydraulic Research Institute, 210029, Nanjing, Jiangsu,China*
[2]*State Key Laboratory of Hydrology-Water Resources and Hydraulic Engineering, 210098, Nanjing,Jiangsu,China*

(Received January 12, 2016, Revised February 15, 2016, Accepted April 15, 2016)

Abstract. In order to observe the internal damage of concrete in real time, we introduced acoustic emission nondestructive detecting technology into a series of fracture tests; the test results revealed the whole process that concrete undergoes when it sustains damage that leads to failure, according to the change rules of the acoustic emission parameters. The results showed that both the initiation and unstable loads can be accurately determined using the abrupt change of the acoustic emission rate curves and the turning point of the acoustic emission parameters' accumulative curves. The whole process, from damage to failure, includes five phases, beginning with damage, such as cracking, a stable crack growth process, a critical unstable stage, and unstable propagation. The brittle fracture characteristics of concrete change when steel bars are joined, because the steel bars and the concrete structure bond, which causes an increase in the acoustic emission signals within the fracture process of the reinforced concrete. The unstable propagation stage is also extended. Our research results provide a valid methodology and technical explanations, which can help researchers to monitor the cracking process of concrete structures, in real time, during actual projects.

Keywords: concrete; reinforced concrete; damage and fracture process; acoustic emission parameters; experimental study

1. Introduction

Acoustic emission (AE) is commonly defined as the transient elastic strain waves within a material that are caused by a distortion of the localized load. In other words, AE is the relaxation process that energy undergoes when the energy state transfers from an upper to a lower stage, which contributes to non-uniform stress distribution within the given materials (Bentahar and Gouerjuma 2013). The AE technique is a dynamic, nondestructive testing method, which can be utilized to assess the damage of materials and structures according to their elastic waves (Muralidhara *et al.* 2012). Additionally, the AE technique has two distinct advantages compared to other custom detection methods; one is its dynamic and real-time characteristics, the other is that it is less invasive for the structural system.

*Corresponding author, Ph.D., Email: xqfan@nhri.cn

http://www.techno-press.org/?journal=cac&subpage=8 ISSN: 1598-8198 (Print), 1598-818X (Online)

The AE technique has been employed in numerous applications to assess the damage characterization of different materials and processes (Shiotani *et al*. 2013), including concrete and large structures (Schechinger and Vogel 2007). Obert and Hodgson studied the effects of AE on various engineering materials in 1941 and 1942, respectively, and they predicted the rate of rock mass failure during excavation processes. In 1950, a German researcher discovered the "Kaiser" effect, in which the AE phenomena were irreversible (Chao Wang *et al*. 2011). Wells studied the relationships among the compressive strength, the elastic modulus, the Poisson's ratio, the tensile splitting strength and the AE signals for 4 groups of cylinder specimens with different aggregates. Considering the AE parameters, Chen obtained the calculating formula for the critical stress-intensity factor and the critical crack opening displacement. Farahat *et al*. (1995) derived the relations between concrete stress and AE parameters, and further illustrated the relationship between the AE activity and the interior damage sustained by the concrete. Gostautas *et al*. (2005) suggested a mechanical model, which can be used to evaluate the damage degree and the strength grade of the concrete material. Using the quantitative analysis of the AE events, Tetsuya Suzuki *et al*. (2010) studied the fracture mechanism of concrete. Shahiron (2013) used the AE parameters, which included its amplitude, rise time, average frequency and signal strength, in order to classify the sustained damage and determine the damage level. Hu *et al*. (2013) research utilized the two-dimensional and three-dimensional orientation diagrams of the AE signals, taken from AE tests, to establish the constitutive relationship between damage and fracture.

The failure process found in concrete, using a three-point bending (TPB) beam, under static loading conditions, is as follows: primary micro cracks and defect cracks appear, then grow into the micro crack area at the tip of the initial cracks; the crack then gradually extends, and finally develops into an instability failure (Aggelis *et al*. 2011). In the actual experiment, the damage-failure inside the concrete samples cannot be directly reflected; therefore, the test results lag, so any inaccuracy in the test process cannot be promptly corrected. Therefore, this paper explores how to: obtain the damage conditions of the concrete during an experiments in real time, track the data to handle the changing rules, reflect upon the process, and apply the results into a practical project, in order to provide a necessary control method for observing the cracking process of concrete. Ultimately, this paper reveals the whole process of concrete damage and fracture through real-time and dynamic observation, and presents a new technique for nondestructive damage and fracture testing for concrete.

2. Experimental program

2.1 Test specimens

When studying the fracture process of concrete using an AE technique, the TPB beam is the best loading way to utilize (Muralidhara *et al*. 2014), because of the constant loading point, the relatively concentrated damage zone and growing region, the relatively simple damage modes and mechanisms, and the pure AE signals. In order to effectively monitor the damage development process of concrete, the specimens used in this study were 100×100×400(mm) in size, including normal concrete and reinforced concrete. The initial crack of specimens is formed using a 2 mm thick steel plate, which has 30-degree angles on one side. The length of the initial crack is 80mm, to ensure that the initial seam height ratio is 0.4.

In this research, all specimens were fabricated using commercial concrete, approved by the

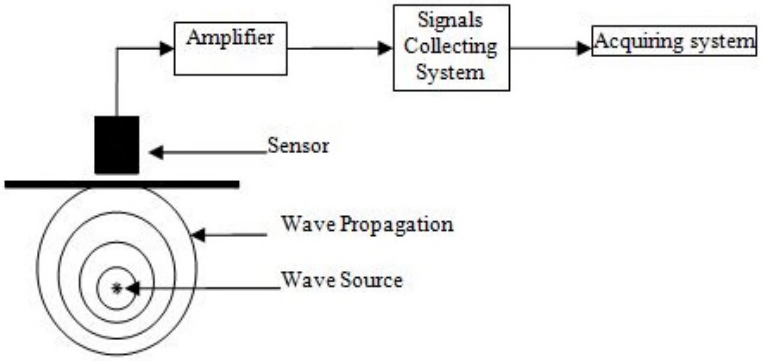

Fig. 1 the fundamentals of acoustic emission technology

concrete association. The ratios of the mass of the water used to create the different cement mixtures were 0.31 (wherein the compressive strength is 29.7 MPa) and 0.5 (wherein the compressive strength is 69.2 MPa). The maximum size of the aggregate was 31.5mm and the coarse aggregate used in this study was river gravel, commonly used in some construction industries. The specimens were de-molded 2 days after casting and were then cured by covering the molds with wet straws for 28 days; afterwards, they were naturally cured in the laboratory. The pre-embedded steel plates were pulled out for five to eight hours per day, based on the actual situation, which was determined by the water to cement ratio, specimen size, initial crack length, and concrete hardening. The various specimens were cast in the same manner from the same batch of concrete.

2.2 Experimental set-up

The 8-channel SAMOSTM AE meter was produced by an American company called Acoustic-mechanical; the system uses modern digital signal processing theory, which happens to be the most advanced AE processing system. When the concrete suffers from internal or external loads, the strain energy can be released via elastic waves. The elastic waves are transmitted to the surface, which causes vibrations. The AE sensors on the surface of the concrete cause deformations, because of the vibrations, and they develop electrical charges. The high-precision chip produces elastic deformations and forms piezoelectric effects under the electric fields. The piezoelectric effect converts the vibrations into voltage signals and indicates what the parameters or pulses are by amplifying and handling the signals. This is the working principle of the AE meter, which accepts and processes the elastic waves.

AE works using sound-electricity transformations, signal amplification, signal processing, recording and displaying the data, explaining and assessing the data, and so on, as shown in Fig. 1.

We polished the surface on which we placed the AE sensors, in order to receive higher quality AE signals and avoid outside interference. Then, we coated the surface with a thin layer of Vaseline as coupling medium. The 8 acoustic emission sensors were installed on the specimen's two symmetry sides as shown in Fig. 2, the number in the brackets indicates that the AE sensors were adhered to their opposites, so that three dimensional positioning was created, and the acoustic emission sensors were fixed on the specimen surfaces with tape to avoid fall-off. The sensors are away from the upper surface or lower surface by 20mm, and on the left side or right side by 150

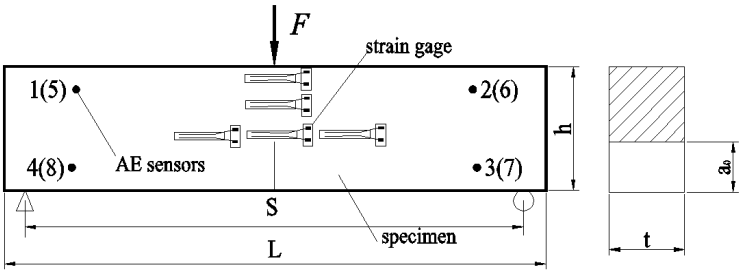

Fig. 2 Arrangement of AE sensors

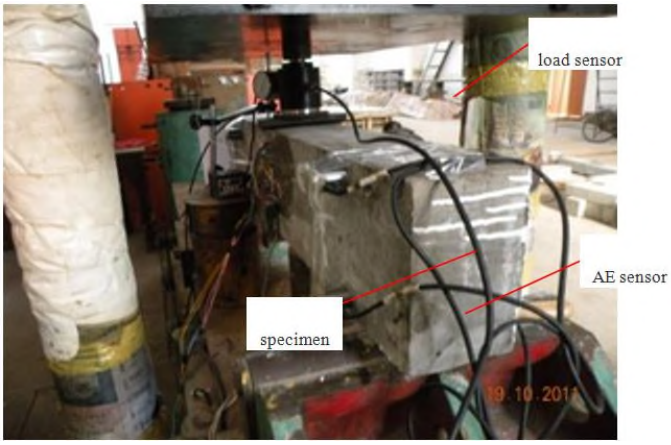

Fig. 3 The picture of AE sensors

mm. Eight AE sensors formed the three-dimensional space. We fixed the sensors using tape to prevent them from falling off. The specimens were loaded at the mid-span using a supported, concentrated load, as shown in Fig. 3.

The data collection includes the strain values, the loads, and the AE signals, as shown in Fig. 4. The loads and strain values were collected with a DH-3817 dynamic strain testing system, using the continuous acquisition mode. The instrument recorded the data every 3 seconds, according to the test photograph shown in Fig. 5. During the AE test, there are two ways to avoid the noise caused by the equipment as well as ambient noise; one is to set the threshold, and the other way is

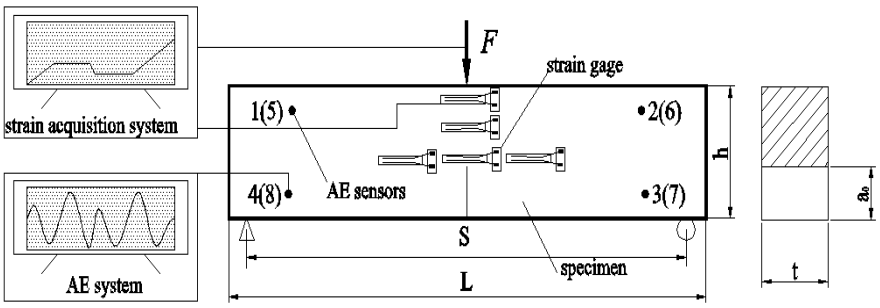

Fig. 4 Scheme of AE experimental set-up

Fig. 5 Photos of AE experimental set-up

to set the filtering frequency. There was a single stress state and the destruction features were obvious to the TPB AE tests, so we filtered the noise through a high sensitive threshold value. The selected threshold value was 40dB and the filtering frequency was set to 20 kHz--100 kHz by idling the machine and the AE frequency range of concrete damage. At the beginning of the damage stage, the AE signals were weak, but the signal strength was increased by setting the gains.

2.3 AE signals

The basic parameters of the AE technique as follows: hits, counts, ringing counts, amplitude, and energy counts, etc.

The AE hits refer to the signals that exceed the threshold and create a channel to get to the data. The hits reflect the total amount and frequency of AE activity, which have two sections: the cumulative counts and count rate.

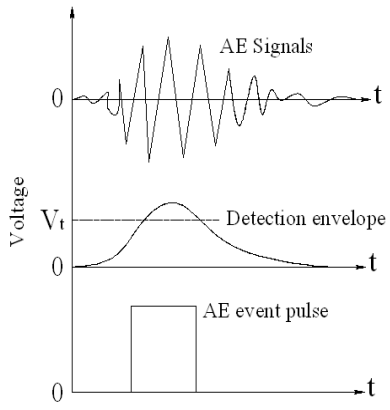

Fig. 6 Photos of AE event count

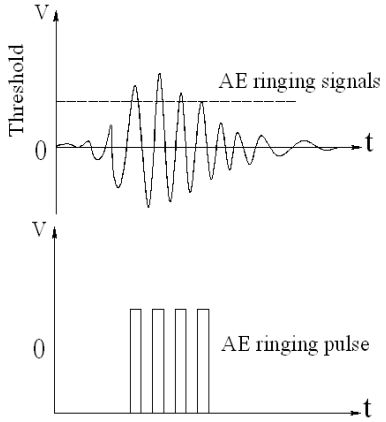

Fig. 7 Photos of AE ringing count

The AE event counts are a commonly used method for processing pulse signals. The AE signals wave as shown in Fig. 6. An event refers to the moment when the wave above the preset threshold voltage can form a rectangular pulse. After the envelope detection technique is applied and an event occurs, the number of pulses is called the event counts. The event count rate and the total event count refer to the counts per unit time and accumulated counts, respectively. Both of them react to the volume and the frequency, which can be used to evaluate the activity and the positioning concentration of the AE sources.

The basic principle of the AE ringing count is shown in Fig. 7. We suggest that researchers should set a threshold voltage, after which, there will be a rectangular pulse when the AE ringing wave exceeds the threshold voltage. The rectangular pulse is called the trigger signal of the ringing count. Each shockwave that exceeds the threshold voltage can be considered as an AE ringing count. The ringing count rate and the accumulated ringing count refer to the ringing count per unit time and the total time, respectively. The AE ringing count roughly reacts to the volume and the frequency, so it is widely used to evaluate the activity of the AE sources. However, the AE ringing count is influenced by the threshold voltage.

The AE amplitude is the maximum swing of the AE event signals waves, expressed in dB. The amplitude directly determines the measurability of an AE event, which is used to identify the category and measure the strength deterioration of the AE wave source.

The AE accumulated energy is the area under the envelope an AE event wave, which includes accumulated energy and energy rated. The AE energy is used to reflect the relative energy and the strength the AE source, which is always insensitive to the propagation feature of the AE wave. The AE energy can replace the AE ringing count and identify the category of the AE wave source.

2.4 Experiment steps

The AE experiment steps to examine concrete damage and fractures are as follows:

(1) For each test series, the samples were formed and maintained according to their own modeling and maintaining methods. We numbered them according to the order. The samples were cured for at least 60 days before the beginning of the experiment.

(2) All of the TPB beams were wiped clean, and we cleaned the surface of the concrete to apply the strain gauge and AE sensors, which were connected the AE meter and data acquisition system.

(3) The method of gluing the strain gauge in place was in accordance with regulations. A thin layer of Vaseline jelly was smeared on the location where we placed the AE sensors, to ensure that the AE sensors were located vertically on the surface of the concrete.

(4) In order to gather the AE signals accurately during the course of the experiments, the lead-break signals were collected to verify the threshold value and wave velocity of the AE systems.

(5) We opened the loading device and began the experiment, and recorded the entire fracture process of the concrete with a high resolution camera when the new crack was visible to the naked eye.

3. Experimental results and analysis of the concrete flexural tests

Fig. 8(a) shows the relationship of the curve between the AE ringing counts rate and the time, whereas Fig. 8(b) establishes the curve between the AE accumulative ringing counts and the time. As we can see from the two pictures, there is no AE signal during the initial loading, so the

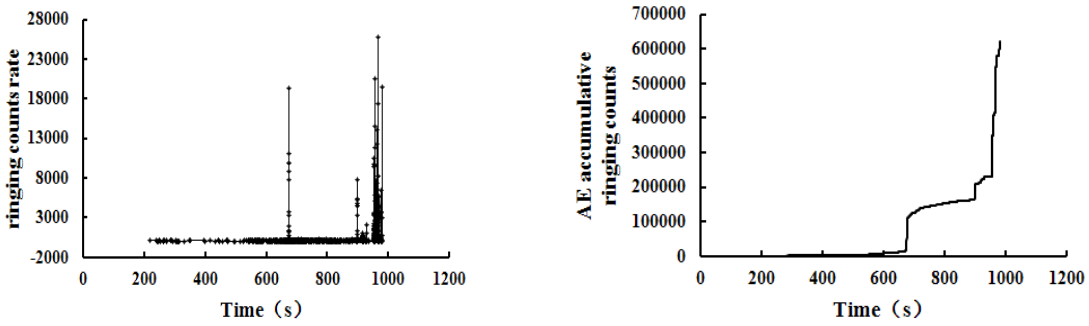

(a) ringing counts rate (b) accumulative ringing counts

Fig. 8 The relative curves between AE ringing counts and time

damage doesn't appear in the concrete. As the load increases, the AE ringing counts rate generates stable signals, and the accumulative ringing counts increase gradually, which is to say that the damage degree of the concrete is consistently enhanced. When the loading time reaches to 680s, the AE ringing counts rate suddenly increases, and the curve between the AE accumulative ringing counts and the time sharply transitions, which means that the concrete is severely damaged. As the time continues from 680s to 950s, both the AE ringing counts rate and the AE accumulative ringing counts steadily change again, and the variation trend is similar to the time from 190s to 680s. Until 950s, the AE ringing counts rate quickly increases again, and the AE accumulative ringing counts suddenly increases once again, these changes indicate that the concrete specimen is destroyed, so the TPB beam quickly breaks and the test ends.

Based on the analyzed results in Fig. 8(a) and Fig. 8(b), the process of damage and fracture for notched concrete TPB beams can be divided into five stages by means of an AE signals, including: (1) There is no damage in the initial phases, nor any AE signals when the load increases, so the TPB beams didn’t suffer any damage. (2) The concrete beam begins to show damage. The AE signals increase homogeneously as the load and the degree of damage to the concrete internal aggravate continuously increase. (3) The concrete structure begins to crack. The degree of damage to the concrete suddenly changes at some point; the ringing counts rate experiences sudden growth, and the slope of the AE accumulative ringing counts curve also increases. (4) This stage of damage degree increases gradually. The AE signals happen continually; the damage degree increases gradually, at the same rate as the second stage, however, the degree of damage is larger. (5) This stage marks the concrete’s instability failure. When the load value reaches its maximum, the AE signals suddenly change once again, and the specimen shows unstable failures.

Professor Xu and Reinhardt (1999) proposed a double-K fracture model, which divided the fracture process of the TPB beam into five parts: when $K < K_{IC}^{ini}$, the initial prefabricated crack does not expand. When $K = K_{IC}^{ini}$, the preformed crack begins to crack initially. When $K_{IC}^{ini} < K < K_{IC}^{un}$, the propagating crack develops steadily. When $K = K_{IC}^{un}$, the propagating crack begins to crack unsteadily. When $K > K_{IC}^{un}$, the crack propagates unsteadily. Based on the AE signals that were shown in Fig. 8(a) and Fig. 8(b), the damage and failure process of the TPB beam can be divided into five stages accordingly. In the first stage, between 0 to 680 seconds, the initial prefabricated crack does not expand. However, at 680 seconds, the preformed crack begins to

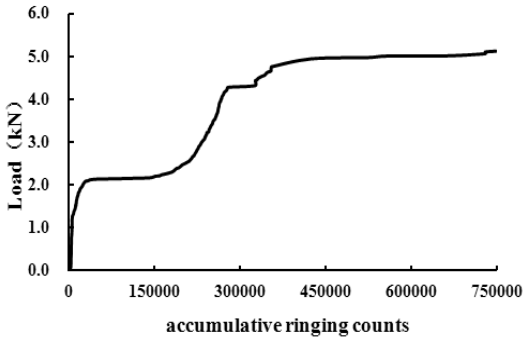

Fig. 9 The relative curves between load and accumulative ringing counts

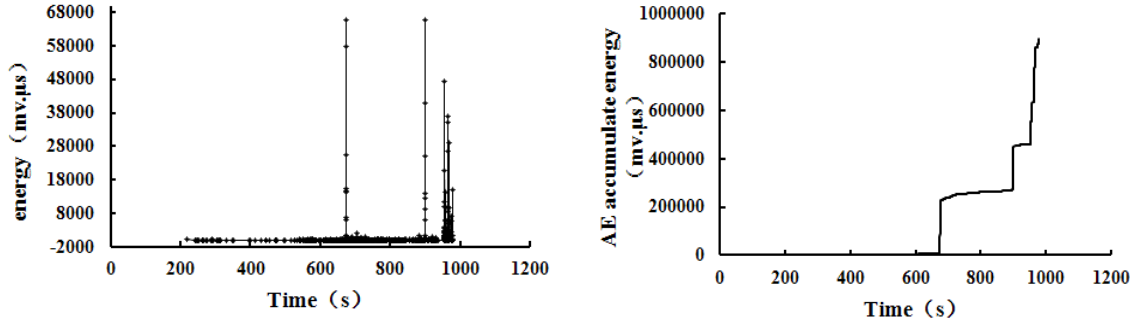

(a) energy (b) accumulate energy

Fig. 10 The relative curves between AE energy and time

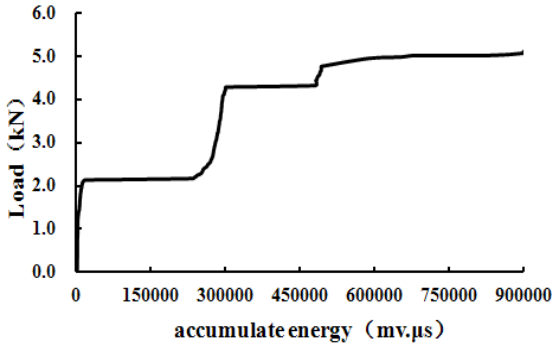

Fig. 11 The relative curves between load and accumulate energy

crack. Between 680 to 950 seconds, the propagating crack develops steadily. At 950 seconds, the preformed crack begins to crack. After more than 950 seconds, the crack propagates unsteadily. That is to say, the processes described across the AE signals and the double-K fracture model is consistent.

In order to calculate the process of double-K fracture toughness (Xu and Reinhardt 1998), the initiation load is absolutely vital for the experiment results. Through analysis, the initiation load and the maximum load can be given accurately using the AE technique. As shown in Fig. 8(a) and

Fig. 8(b), at 680 seconds, the preformed crack begins to crack. At 950 seconds, the propagating crack reaches an unstable state, and the corresponding loads are the initiation load and the maximum load, respectively. However, the load cannot be read out directly from Fig. 8(a) or Fig. 8(b). Accordingly, the relative curves between the loads and the AE accumulative ringing counts are shown in Fig. 9. The two turning points of the curves correspond to the initiation load and the maximum load, respectively.

The change rules of the other AE parameters can also react to the damage and fracture process, with the exception of the ringing counts. Using AE energy as an example, the curves of energy and time, the accumulate energy and time, and the load and accumulate energy are shown in Fig. 10(a), Fig. 10(b) and Fig. 11. As can be seen in the figures, the changing laws of AE energy and time curve are consistent with the curve of the ringing counts and time.

4. Experimental results and analysis of reinforced concrete flexural tests

Similar to the analysis method used for concrete with the AE signals, the change curves of the reinforced concrete AE parameters were shown in Fig. 12(a) and Fig. 12(b). Through analyzing Fig. 12(a), we divided the fracture process of the reinforced concrete TPB beam into six stages based on the AE signals. (1) In the first stage, there are not any AE signals. In the initial stages, the load on the specimen is smaller, and the reinforced concrete has not suffered any damage, so it is impossible see AE signals at this stage. (2) The second stage lasts from the onset of the AE signals to the first signal peak. The number of AE signals increases gradually as the load increases, and the reinforced concrete structure begins to damage; however, the damage degree is very limited relative to the ultimate bearing capacity of the RC structure, so the AE signals are relatively weak. (3) The third stage refers to when the first signals peak. The structure suddenly cracks at some point and the AE signals also change drastically to create the first peak. (4) In the fourth stage, the concrete reaches a stable state after the first signals peak. Because of the fracture process zone of concrete, the cracks propagate slowly after the reinforced concrete cracks and the damage degree gradually increases, but the degree of damage does not change suddenly, so the AE signals increase steadily. (5) The fifth stage occurs when the second signals peak. When the load reaches its maximum value after the reinforced concrete structure cracks at some point, the unstable failure happens accordingly, so the AE signals increase suddenly and form the second peak. (6) The sixth stage happens when destruction occurs after the second signals peak. The fracture process of reinforced concrete is different from that of normal concrete, because of the steel rebar. When the load reaches its maximum value, the reinforced concrete does not experiences instability failure, but the load slowly decreases with time, and the damage degree continuously accumulates until the structure is damaged.

Fig. 12(b) shows the relative curves between AE accumulate ringing counts and time for reinforced concrete. As we can see from the picture, the curves accurately reflect the stages as follows: the first stage (no damage); the second stage (begins to damage); the third stage (the first turning point); and the change rules are not obvious for the remaining sections. In order to analyze the differences and relationship between the fracture processes of reinforced concrete and common concrete, we compared Fig. 8(a) and Fig.12(a) to one another. The AE signals of the concrete are relatively pure (in Fig. 8(a)); however, the AE signals of the reinforced concrete are cluttered (in Fig. 12(a)), which is why the curve between the AE accumulate ringing counts and time is irregular (in Fig. 12(b)), especially in the instability time. Since the rate of AE signals in the

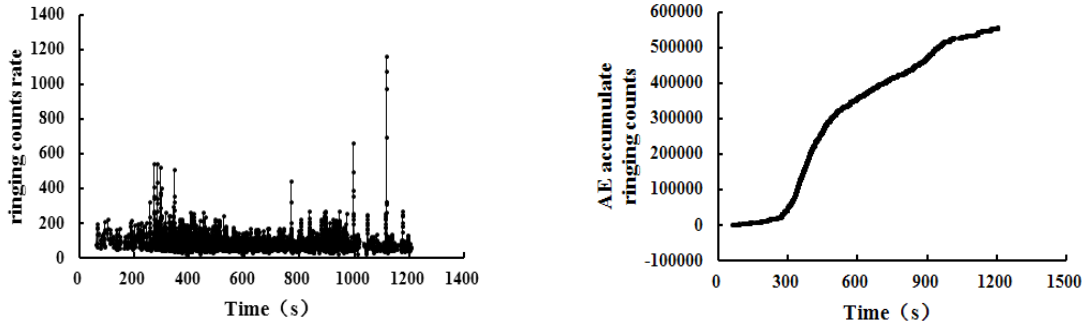

(a) ringing counts rate (b) accumulative ringing counts

Fig. 12 The relative curves between AE ringing counts and time for reinforced concrete

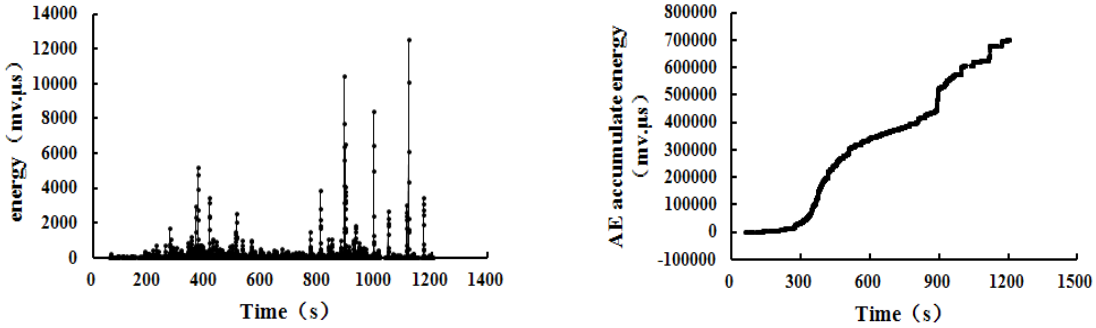

(a) energy (b) accumulate energy

Fig. 13 The relative curves between AE energy and time for reinforced concrete

ringing counts are more cluttered, it is difficult to judge the fracture process in Fig. 12(b). After analyzing the causes, we found that the behavior of brittle failure changes when the steel bars were implanted into the concrete. There are constraining forces between the concrete and the steel bars, so the balanced constraining forces will break constantly as the load increases and sets up a new state of equilibrium. The AE signals are inevitable when the balance is broken, so the AE signals of the reinforced concrete are relatively cluttered.

Except the curves of the AE ringing counts and time, the curves of the AE energy and time for reinforced concrete are shown in Fig. 13(a) and Fig. 13(b), respectively. The AE ringing counts can complement the AE energy. By combining the two curves, the initiation load and the unstable load can be correctly judged, based on the change rules of the reinforced concrete AE signals.

5. Conclusions

This paper analyzed the damage and fracture process of concrete TPB beams based on a new AE technique.

Corresponding to the five failure stages of the concrete double K fracture model, the failure process of the concrete TPB were divided into five stages based on their AE signals: when damage appears, the sample begins to crack, stable crack propagation, and critical instability to unstable

crack propagation, respectively. The critical points of crack and instability can be determined through the sudden changes of the AE rate curves or the turning point of the AE cumulative curves.

The damage and fracture failure process of reinforced concrete is different from the failure process in the common concrete. The addition of steel bar changes the brittle failure of the concrete, and the steel bar binds with the concrete. For these reasons, the AE signals become disorganized in the fracture process of the reinforced concrete; however, the ductility becomes better during the expansion phase of instability. The AE signals of the reinforced concrete then divide the failure process into six stages: namely, no AE signal in the initial phase; the process from the appearance of the AE signal to the first peak; the first peak point; the stable expansion stage after the first peak; the second peak point; and the failure stage after the second peak.

Acknowledgements

This research has been partially supported by the National Funds for Distinguished Young Scientists of China (SN: 51325904); the National Natural Science Foundation of China (SN: 51309163, 51409162 and 51527811); The Natural Science Foundation of Jiangsu Province (SN: BK20140081) and The Project funded by China Postdoctoral Science Foundation (SN: 2014M551624). The authors thank the reviewers for their useful comments and suggestions that helped to improve the paper.

References

Aggelis, D.G., Soulioti, D.V., Sapouridis, N., Barkoula, N.M., Paipetis, A.S. and Matikas, T.E. (2011), "Acoustic emission characterization of the fracture process in fibre reinforced concrete", *Constr. Build. Mater.*, **25**(11), 4126-4131.

Bentahar, M. and Gouerjuma, R.E.(2013), "Monitoring progressive damage in polymer based composite using nonlinear dynamics and acoustic emission", *J. Acoust. Soc. America*, **125**(1), 39-44.

Chen, H.L., Cheng, C.T. and Chen, S.E. (2012), "Determination of fracture parameters of mortar and concrete beams by using acoustic emission", *Mater. Eval.*, **13**(1), 888-894.

Farahat, A.M. and Ohtsu, M. (1995), "Evaluation of plastic damage in concrete by acoustic emission", *J. Mater. Civil Eng.*, **7**(3), 148-153.

Gostautas, R.S., Ramirez, G., Peterman, R.J. and Meggers, D. (2005), "Acoustic emission monitoring and analysis of glass fiber-reinforced composites bridge decks", *J. Bridge Eng.*, **10**(6), 713-721.

Hu, S., Lu, J. and Xiao, F. (2013), "Evaluation of concrete fracture procedure based on acoustic emission parameters", *Constr. Build. Mater.*, **47**, 1249-1256.

Muralidhara, S., Prasad, B.R., Eskandari, H. and Karihaloo, B.L. (2010), "Fracture process zone size and true fracture energy of concrete using acoustic emission", *Constr. Build. Mater.*, **24**(4), 479-486.

Muralidhara, S., Prasad, B.R., Eskandari, H. and Karihaloo, B.L. (2010), "Fracture process zone size and true fracture energy of concrete using acoustic emission", *Constr. Build. Mater.*, **24**(4), 479-486.

Schechinger, B. and Vogel, T. (2007), "Acoustic emission for monitoring a reinforced concrete beam subject to four-point-bending", *Constr. Build. Mater.*, **21**(3), 483-490.

Shahidan, S., Pulin, R., Bunnori, N.M. and Holford, K.M. (2013), "Damage classification in reinforced concrete beam by acoustic emission signal analysis", *Constr. Build. Mater.*, **45**, 78-86.

Shiotani, T., Bisschop, J. and Van Mier, J.G.M. (2003), "Temporal and spatial development of drying shrinkage cracking in cement-based materials", *Eng. Fract. Mech.*, **70**(12), 1509-1525.

Suzuki, T., Ogata, H., Takada, R., Aoki, M. and Ohtsu, M. (2010), "Use of acoustic emission and X-ray computed tomography for damage evaluation of freeze-thawed concrete", *Constr. Build. Mater.*, **24**(12), 2347-2352.

Wang, C., Zhang, Y. and Ma, A. (2010), "Investigation into the fatigue damage process of rubberized concrete and plain concrete by AE analysis", *J. Mater. Civil Eng.*, **23**(7), 953-960.

Xu, S. and Reinhardt, H.W. (1998), "Crack extension resistance and fracture properties of quasi-brittle softening materials like concrete based on the complete process of fracture", *Int. J. Fract.*, **92**(1), 71-99.

Xu, S.L. and Reinhardt, H.W. (1999), "Determination of double-K criterion for crack propagation in quasi-brittle materials, part II: analytical evaluating and practical measuring methods for three-point bending notched beams", *Int. J. Fract.*, **98**(2), 151-177.

CC